International Journal of Engineering Research & Technology (IJERT)
ISSN: 2278-0181
Vol. 5 Issue 12, December-2016

Spectral Feature of Sampling Errors for Directional Samples on Gridded Wave Field

Ming Luo, Igor G. Zurbenko
Department of Epidemiology and Biostatistics
State University of New York at Albany
Rensselaer, USA

***Abstract*—This paper discussed the underlying mechanism for a kind of sampling errors for directional samples in gridded wave fields. We demonstrated that these sampling errors are periodic signals with seesaw like waves; their fundamental frequencies and dominated frequencies are functions of the sampling directions. When this kind of sampling errors act on directional periodogram, their modulation effects can be approximately predicted. Related results can be used to identify the source of unusual periodogram spikes in the wave identification analysis.**

Keywords*—Gridded wave fields; spectrum; periodogram; directional sampling; discretization; sampling errors; spatial wave image; modulation effect.

I. INTRODUCTION

Spatial signal data often comes in the form of values plus spatial coordinates. For example, regularly sampled spatial data usually are organized as arrays, for which each dimension corresponds to grid or lattice coordinate of the spatial points. In many cases, irregularly sampled data could also be transformed into their discrete version through gridding the spatial coordinates and aggregating observation values. Gridded data can simplify the problem and is suitable for spectral analysis [1, 2], therefore it is common to see in engineering, acoustics, physical oceanography, astronomy, climate change [3, 4], oceans waves alarm and many other application fields.

In this paper, we focus on the situations in which spatial signal data are collected on a pre-defined set of grid points, i.e., gridded wave fields. Since the spatial coordinates of data are fixed in advance, it caused some special issues that it may not be a problem when data can be re-aggregated and the grid can be re-defined. Sampling error for data samples on the lines along a given direction is one of such issues. Usually we have to deal with difference frequencies of oscillations along the sampling line. Unit speed along the line generates frequency along x and along y. Their spectral space is the superposition of these different frequencies. Those signals, noises, and related sampling error effects make wave surface complicated. Here we will provide an analytical formula to describe the sampling errors' spectrum for directional samples on gridded wave field; then the phase modification effects of sampling errors on the periodogram of directional samples will also be discussed.

II. SAMPLING ERRORS FOR DIRECTIONAL SAMPLES

Suppose a wave field is defined on the grid $\mathbf{G} = \{(x, y)\}$, where $x = 1, 2, \ldots, d_x$, $y = 1, 2, \ldots, d_y$; d_x and d_y are integers. Don't lose generality, we assume that the data values are observed on grid points, i.e., the regular sampling intervals of wave signals are all 1 unit on both x and y direction. Then, the observations for the combination effects of a group of spatial waves $\mathbf{W} = \{w_u(x, y)\}$ on $\mathbf{G}$ can be represented by a data array $\mathbf{D}$ with dimension (d_x, d_y); the effects of background noises, which are limited to homogeneous Gaussian Noises in this paper, should also be included in array $\mathbf{D}$, i.e., $\mathbf{D}$ represents the gridded wave field on $\mathbf{G}$.

Now we are interested in checking the periodogram for data series ordered along a given direction θ. Assume for any sinusoid wave $w_u(x, y)$ in $\mathbf{W}$, $w_u(x, y)$ is wide-sense stationary on grid $\mathbf{G}$. It means that $w_u(x, y)$ has the same distributions for frequency and direction on the gridded wave field. Therefore, a data series on a line along angle θ is a directional sample of the gridded wave field. In general cases, the sampling line does not necessarily pass through the grid points of the wave field; therefore we have to replace the real wave values with observations on the nearest grid points. The differences for the coordinates of data values are the sampling errors for directional samples on the gridded wave field.

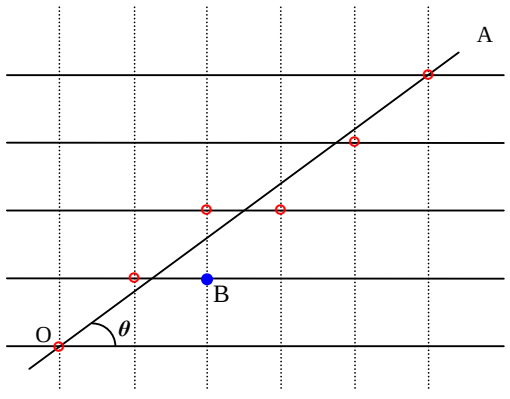

Fig. 1. Sampling errors along sampling direction θ

International Journal of Engineering Research & Technology (IJERT)
ISSN: 2278-0181
Vol. 5 Issue 12, December-2016

Definition 1: For a sampling line along direction angle θ in the gridded wave field **D**, its sampling errors on **D** are:

$$e(\theta; t) = tan(\theta)t - round(tan(\theta)t), \text{ from y direction} \quad (1a)$$

$$e(\theta; t) = t/tan(\theta) - round(t/tan(\theta)), \text{ from x direction} \quad (1b)$$

where *round*(.) is the rounding function; $t \in \mathbf{Z}$, t is the index of points on the sampling line.

There are two feasible ways to define the sampling errors. For sampling errors from perspective along y direction, we can take $t = x + x_0$; otherwise, $t = y + y_0$. Here x_0 and y_0 are the coordinate for the sampling line intersect with the axis. We often need only select one of them to use in practice. As illustrated in Fig. 1, if the red circles are gridded samples on the line, the intersections with grid lines along x or y direction can be chosen as the real wave values, corresponding to Eq. 1a and 1b, respectively. For perspective along y direction, the highest absolute values of the rounding errors appear in the middle of line segment OA; but usually it is less than half of the grid interval. The sampling errors usually are a periodic movement with zero mean and can be approximated as:

$$e(t) \approx \sum_{m=1 \text{ to } M} e_m(t) = \sum_{m=1 \text{ to } M} A_m \sin(2\pi f_m t + \varphi_m) \quad (2)$$

Here t can be viewed as the sampling steps on direction θ. Next, we will show that the frequencies of the major components of $e(t)$, denoted by f_m in Eq. 2, are only related to direction θ.

Proposition 1: For a sampling line along direction θ ($0 \le \theta \le \pi$) on grid $\mathbf{G} = \{(x, y)\}$, $x \in \mathbf{Z}$, $y \in \mathbf{Z}$, suppose $|\tan(\theta)| = a/b$, $a \in \mathbf{N}$, $b \in \mathbf{N}$, a and b don't have common factors; then the fundamental frequency for the sampling errors on direction θ is $1/b$.

Proof: The proof is straightforward. For perspective along y direction, since b is integer, if we starting from a grid point O on the x-axis, for where sampling error is zero, after each b steps along θ we will end in another grid point with zero sampling error. Thus b steps should be one period of $e(t)$, i.e.,

$$e(t + k \cdot b) = e(t), \text{ for all } k \in \mathbf{Z}. \quad (3)$$

In fact, there doesn't exist a period $c > b$, $c \neq k \cdot b$, $k \in \mathbf{Z}$. Otherwise, it will conflict with the condition $|\tan(\theta)| = a/b$. Therefore, $1/b$ is the fundamental frequencies of $e(t)$. Similarly, Proposition 1 is also true for sampling errors from the perspective of x direction.

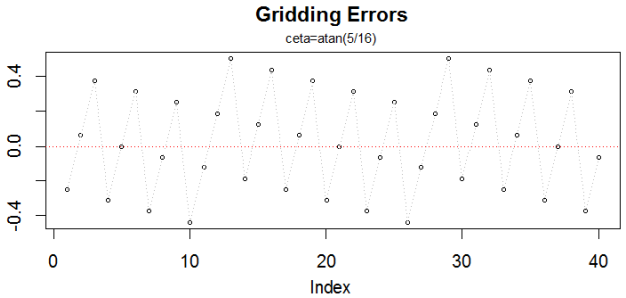

Fig. 2. Sawtooth waves of sampling errors along direction *atan*(5/16)

Based on Proposition 1, we can see that $1/b$, $2/b$, …, a/b all are possible frequencies for f_m in Eq. 2. Also, φ_m are the same constant for all $m = 1, ..., M$.

$$e(t) \approx \sum_{m=1 \text{ to } M} e_m(t) = \sum_{m=1 \text{ to } M} A_m \sin(2\pi \cdot m \cdot t/b + \varphi) \quad (4)$$

It would be useful in practice if we can know in advance the dominate frequency of $e(t)$, or say, which part of $e(t)$ has the most power or the largest A_m.

Proposition 2: For a sampling line along direction θ ($0 \le \theta \le \pi$) on grid $\mathbf{G} = \{(x, y)\}$, $x \in \mathbf{Z}$, $y \in \mathbf{Z}$, if $|\tan(\theta)| = a/b$, $a \in \mathbf{N}$, $b \in \mathbf{N}$, a and b don't have common factors. Suppose f_* has the largest power among all the frequency components for sampling errors along direction θ, then f_* can be decided as following:

$$E(f_*) = min(|tan(\theta)|, 1-|tan(\theta)|), \text{ from y direction} \quad (5a)$$

$$E(f_*) = min(1/|tan(\theta)|, 1-1/|tan(\theta)|), \text{ from x direction} \quad (5b)$$

Proof: We first check the sampling errors from perspective along y direction, as showed in Fig. 1. Considering the zero-crossings of the sampling error $e(t)$, it can only happen when the sampling line crosses the line of $y = 0.5k$, $k \in \mathbf{Z}$. If $a/b < 0.5$, for each time the sampling line crosses the line of $y = 0.5k$, $e(t)$ changes its sign. Thus $e(t)$ has $2a$ zero-crossings in b steps of one period, including the zero value on the starting point.

For $0.5 \le a/b < 1$, one "step" may cross more than one line of $y = 0.5k$, $k \in \mathbf{Z}$. So it is not easy to count the zero-crossings. But we can consider the flowing two series: $(a/b)k$ and $(1-a/b)k$, $k = 2, ..., b-1$. The first is the sampling series itself, while the later is the difference between sampling line of direction $\pi/4$ and θ. The rounding errors for these two series changes at the same time, or say, they have the same zero-crossings signal. In fact, we can rewrite the sampling errors $e(t)$ as following:

$$\begin{aligned} e(k) &= round(ka/b) - ka/b = k - ka/b + round(ka/b) - k \\ &\equiv (1 - a/b) \cdot k + round(k \cdot a/b - k), \text{ if } -0.5 \equiv 0.5 \text{ for } e(t) \\ &= (1 - a/b) \cdot k - round((1 - a/b) \cdot k) \end{aligned} \quad (6)$$

It means the rounding errors of series $(a/b)k$ is actually the negative of rounding errors of series $(1 - a/b)k$, $k = 2, ..., b-1$. The condition in this equation can also be $1 \equiv 0$ or $-1 \equiv 0$. Since $(1 - a/b) < 0.5$, following the inference of previous paragraphs for $a/b < 0.5$, we can conclude that $e(t)$ changes its signs for $2(1 - a/b)$ times from point O to A in Fig. 1.

Summarizing two situations, frequency component of a/b decides the zero-crossings of $e(t)$. Now we can use the zero-crossings to detect the "pitch" of the sampling error signal. The condition is 1) no noise, and 2) the wave shape of the signal is clear. Basically, the sampling errors are sawtooth waves of period of b/a plus a smaller sawtooth adjustment of period b, as showed in Fig. 2. The Fourier transform of sawtooth wave [5] with frequency f is –

$$x_{saw}(t) = A/2 - (A/\pi) \sum_{k=1 \text{ to } \infty} (-1)^k \sin(2\pi k f t)/k \quad (7a)$$

$$x_{revsaw}(t) = 2A/\pi \cdot \sum_{k=1 \text{ to } \infty} (-1)^k \sin(2\pi k f t)/k \quad (7b)$$

Therefore, the frequency of sawtooth waves is the dominated frequency of its Fourier series, reflected by the frequency of the zero-crossings signal. In other words, $e(t)$ is the summary of harmonic signals of $\sin(2\pi ta/b)$ and $\sin(2\pi t/b)$, and frequency $f_* = a/b$ should have the largest amplitude among $e_m(t)$, $m = 1, ..., M$. Considering the aliasing effects, Eq. 5a holds. The situation of Eq. 5b can be proofed similarly.

International Journal of Engineering Research & Technology (IJERT)
ISSN: 2278-0181
Vol. 5 Issue 12, December-2016

Remark: For the situation of b is an even integer, the dominate frequency of $e(t)$ also will be affected by the method to deal with the duels in rounding numbers, i.e., the cases with value -0.5 and 0.5. If the allowed rounding errors are limited to [-0.5, 0.5) or (-0.5, 0.5], Eq. 5a and 5b are still true for b as even integers. This is also the condition for Eq. 6.

Fig. 3 is an example of the periodogram of sampling errors for sampling lines on the gridded wave field. The dominated frequency of sampling errors is 5/16, other spectrum peaks are its harmonic or harmonic of $sin\ (2\pi t/16)$. This periodogram plot is consistent with Eq. 5.

III. Modulation Effects of Sampling Errors

When sampling errors interact with spatial waves in the wave field, the wave signal would be modulated. Generally, on the periodogram for sampling lines on gridded wave field, the spectral spikes caused by sampling errors usually are not strong and could be smoothed out as noise effects. In some extent, these modulation effects can be anticipated.

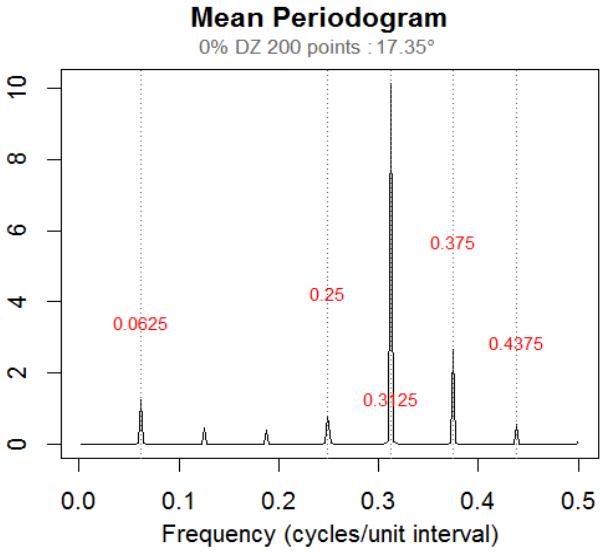

Fig. 3. Directional periodogram of sampling errors along direction *atan*(5/16)

Proposition 3: For continuous sinusoid wave $w(x, y)$, if the wave frequency for sample points on the sampling line along direction θ ($0 \le \theta \le \pi$) is ν_d, then the gridded samples of the same sampling lines will have dominated frequency ν_d and additional signals around $\nu_{de1} = \nu_d \pm f_*$ and $\nu_{de2} = \nu_d \pm 2 \cdot f_*$, where f_* is the dominated frequency of the sampling errors.

Proof: Suppose sinusoid wave $w(x, y)$ propagates along direction β ($0 \le \beta \le \pi$); its projection on the sampling lines along direction θ ($0 \le \theta \le \pi$) is $w_\theta(x) = sin(\omega_d x + \psi)$. The sampling errors $e(t)$ is from perspective along y direction, then $e(x) \cdot sin(\beta)$ is the part act on the wave direction. The wave signal $w_\theta(x)$ after gridding is denoted as $w_{e,\theta}(x)$, then we will have the following equation:

$$w_{e,\theta}(x) = sin(\omega_d (x + e(x) \cdot sin(\beta)) + \psi)$$
$$= sin(\omega_d x + \psi + sin(\beta) \cdot \omega_d \sum_{m=1 \text{ to } M} e_m(x)) \quad (8)$$

This means that the sampling errors will modulate the phase of the wave signal. It can also be viewed as a change of the frequency of the signal. Since the analytical result is complicated, we will focus on the spectral behavior of major components of $w_{e,\theta}(x)$. We can consider the effects of $e_m(t)$, $m = 1, ..., M$, separately.

$$w_{em,\theta}(x) = sin(\omega_d x + \psi + sin(\beta) \cdot \omega_d \cdot e_m(x)) =$$
$$= sin(\omega_d x + \psi) cos(sin(\beta) \cdot \omega_d \cdot e_m(x)) +$$
$$cos(\omega_d x + \psi) sin(sin(\beta) \cdot \omega_d \cdot e_m(x)) \quad (9)$$

In our cases, $e_m(t)$ have small amplitudes, $\Delta = sin(\beta)\ \omega_d A_m \le 0.707 \cdot 2\pi \cdot 0.5 \cdot 0.5 \approx \pi/2.828$, therefore we have

$$cos(\Delta \cdot sin(\omega_m x + \varphi_m)) \approx 1 - \gamma(\Delta) + \gamma(\Delta) cos(2\omega_m x + \varphi_m) \quad (10)$$
$$sin(\Delta \cdot sin(\omega_m x + \varphi_m)) \approx \zeta(\Delta) sin(\omega_m x + \varphi_m) \quad (11)$$

where $\gamma(\Delta)$ and $\zeta(\Delta)$ are functions of Δ. Usually, Eq. 11 works best when $\Delta < \pi/3$ or smaller, but here it is good enough for revealing the spectral characteristic of Eq. 9.

$$w_{em,\theta}(x) \approx sin(\omega_d x + \psi)[1 - \gamma(\Delta) + \gamma(\Delta) cos(2\omega_m x + \varphi_m)] +$$
$$cos(\omega_d x + \psi) \zeta(\Delta) sin(\omega_m x + \varphi_m)$$
$$= sin(\omega_d x + \psi)[1 - \gamma(\Delta)] +$$
$$\gamma(\Delta)[sin((\omega_d + 2\omega_m)x + \psi + \varphi_m) + sin((\omega_d - 2\omega_m)x + \psi - \varphi_m)]/2 +$$
$$\zeta(\Delta)[sin((\omega_d + \omega_m)x + \psi + \varphi_m) - sin((\omega_d - \omega_m)x + \psi - \varphi_m)]/2 \quad (12)$$

The approximated result is like an amplitude modulation. Beside the "carrier" frequency ω_d, new frequency component $\omega_d \pm \omega_m$ and $\omega_d \pm 2\omega_m$ have been introduced by modulation of sampling errors. Similarly, Eq. 12 also holds for sampling errors from perspective of x direction.

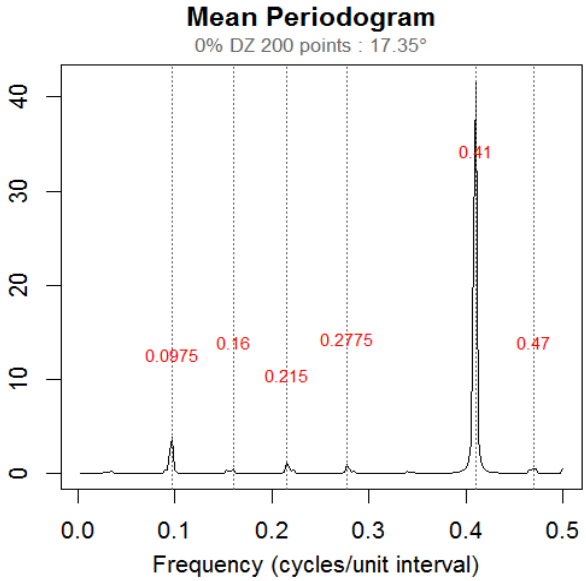

Fig. 4. Modulation effects of sampling errors. Signals: sin ($2\pi \cdot 0.4 \cdot t$) along 30°; noise: none; sampling direction: *atan* (5/16)

When $\Delta \to 0$, $\zeta(\Delta) >> \gamma(\Delta)$, because they are function of Δ in different order: for $\Delta < \pi/3$, $\zeta(\Delta) \approx c_1\Delta$, $\gamma(\Delta) \approx c_3\Delta^2$. The

International Journal of Engineering Research & Technology (IJERT)
ISSN: 2278-0181
Vol. 5 Issue 12, December-2016

modulation effects of $\omega_d \pm \omega_m$ is much stronger than that of $\omega_d \pm 2\omega_m$ when Δ is small. In may cases, we only need to consider the dominated frequency $f_* = \omega_m /2\pi$, and its effects of $v_d \pm f_*$. According to Carson's Rule for Phase Modulation, most of the energy of the modulated signal is contained within the bandwidth of $2(h+1)\omega_m$, and h is the peak phase deviation. In our case, $h \leq \pi/2$. This is consistent with conclusion of Eq. 12

IV. Directional Periodogram Examples

This section will illustrate some examples for the spectrum of directional samples modulated by sampling errors. First, let take a look at the modulation effects for the example exhibited in Fig. 3. Here $v_d = 0.41$, $f_* = f_1 = 5/16 = 0.3125$, and $f_2 = 0.375$, $f_3 = 0.0625$, $f_4 = 0.4375$. For sampling errors modulated signal, the major expected spectral spikes are at 0.41, and other spikes are all consistent with Fig. 4.

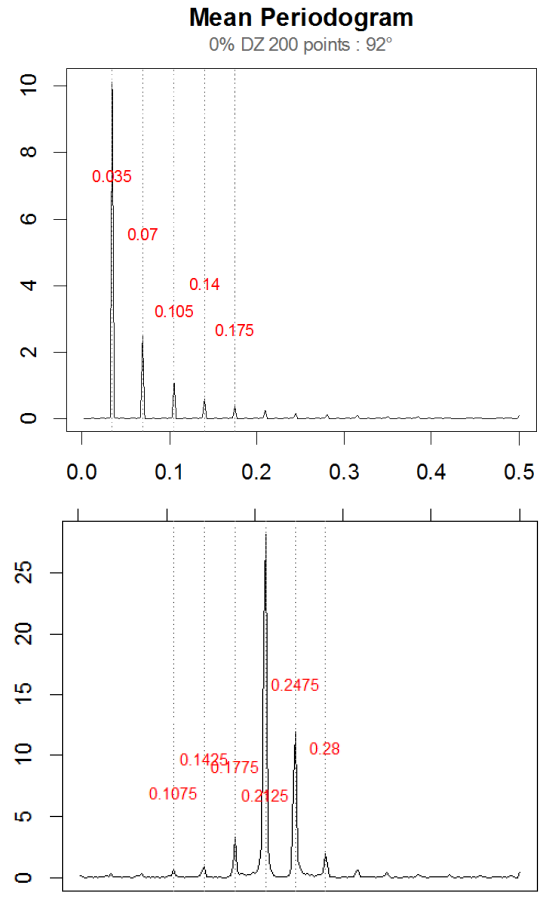

Fig. 5. Periodogram of sampling errors (upper) and the modulated wave (bottom). Signals: sin $(2\pi \cdot 0.45 \cdot t)$ along 30°; noise: none; direction $\theta = 92°$.

Fig. 5 exhibits another example of sampling errors and the modulation effects. For the given sampling line, $E(v_d) = 0.45 \cdot cos(92°\text{-}30°)/sin(30°) = 0.2114$. Following Eq. 1, we will have $f_* = tan(2\pi/180) = 0.035$; the modulated signal have spikes at $f_c + f_* = 0.246$ and $f_c - f_* = 0.176$, $f_c + 2f_* = 0.281$, $f_c - 2f_* = 0.141$. The detected results fit the formula very well.

Fig. 6 is another example: 2 sinusoid waves propagate along direction 30° and -30° in a 400 x 400 wave field; the frequency is 0.4 and 0.05, respectively. Their amplitudes are 1 and 1.5; while the Gaussian noise is $N(0, 10^2)$. The signals are buried in the noises. Fig. 6 is the periodogram for directional samples along angle $\theta = 15°$. Please notice that there is a small peak around frequency 0.3325. This is the modulation effect of sampling errors act on periodogram spike at frequency 0.4: it is not significant and can be smoothed out, thus it is not marked as wave spectral signal in the plot.

However, in practice there are cases for which sampling errors are not negligible, especially when wave frequencies are large and noise levels or smoothing levels are relatively low. As in Fig. 7, beside the expected dominated frequency at 0.4, there are a series of small frequency peaks caused by sampling errors; the spike at 0.1767 is not just a small peak.

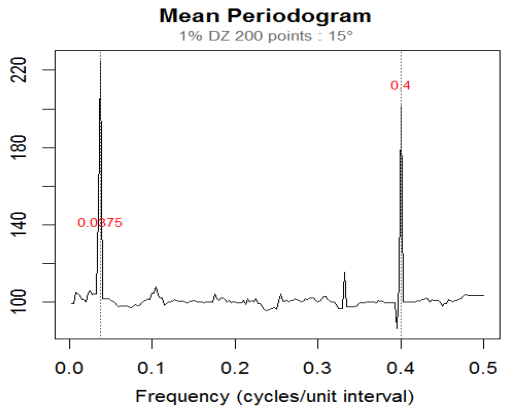

Fig. 6. Periodogram for gridded directional samples along 15°. Signals: $sin(2\pi \cdot 0.4 \cdot t)$ along 30°; $1.5 \cdot sin(2\pi \cdot 0.05 \cdot t)$ along -30°; noise ~ $N(0, 100)$.

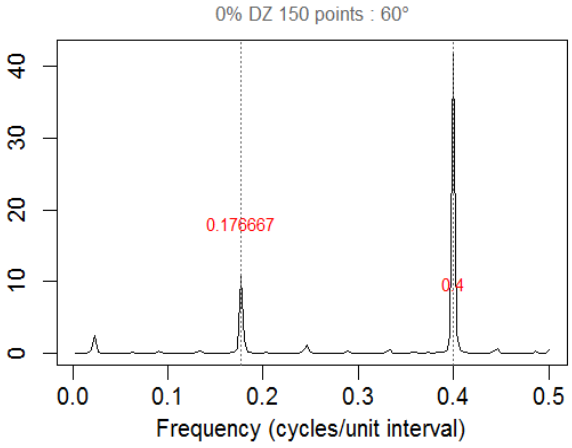

Fig. 7. Effects of sampling errors for directional periodogram along 60°. Signals: $sin(2\pi \cdot 0.4 \cdot t)$ along 30°; noise: none

V. Linear Interpolation of the Wave Signal

Sometimes, the method of linear interpolation is used to remedy the effects of sampling errors. A typical algorithm is interpolating by weighting based on distances of real value to grid points. Suppose the grid interval is 1 on both x and y

International Journal of Engineering Research & Technology (IJERT)
ISSN: 2278-0181
Vol. 5 Issue 12, December-2016

direction, and we denote the interpolated signal as $w_{e',\theta}(t)$ on the sampling line along direction θ, then the algorithm is:

$$w_{e',\theta}(x) = \alpha \cdot w(x, floor(\tan(\theta)\cdot(x+x_0))) + (1-\alpha)\cdot w(x, ceiling(\tan(\theta)\cdot(x+x_0))) \quad (13)$$

where $\alpha = |\tan(\theta)\cdot(x+x_0) - ceiling(\tan(\theta)\cdot(x+x_0))|$, $x \in \boldsymbol{Z}$, for perspective of y direction.

$$w_{e',\theta}(y) = \alpha \cdot w(floor(\tan(\theta)\cdot(y+y_0))), y) + (1-\alpha)\cdot w(ceiling(\tan(\theta)\cdot(y+y_0))), y) \quad (14)$$

where $\alpha = |\tan(\theta)\cdot(y+y_0) - ceiling(\tan(\theta)\cdot(y+y_0))|$, $y \in \boldsymbol{Z}$, for perspective of x direction.

Notice that the frequencies of α and (1 - α) is actually the frequency of sampling errors $e(\theta; t)$ before interpolation; the frequencies of $w(x, floor(\tan(\theta)(x+x_0)))$ and $w(x, ceiling(\tan(\theta)(x+x_0)))$, as while as $w(floor(\tan(\theta)(y+y_0)), y)$ and $w(ceiling(\tan(\theta)(y+y_0)), y)$ all have the same frequency as sampling errors $e(\theta; t)$, which has $f_* = |\tan(\theta)|$. However, their phases are quite different to each other. Here we don't further extend the formula. An important fact is that linear interpolation of the wave signal cannot totally eliminate the effects of the dominated frequency of sampling error f_*, but it can largely diminish the effects of other harmonic frequency of f_*. In fact, linear interpolation will introduce an amplitude modulation of wave signal with frequency f_*. Thus this method will reduce the power of the wave signal; but the effect of f_* will still appear in the periodogram (see Fig. 8).

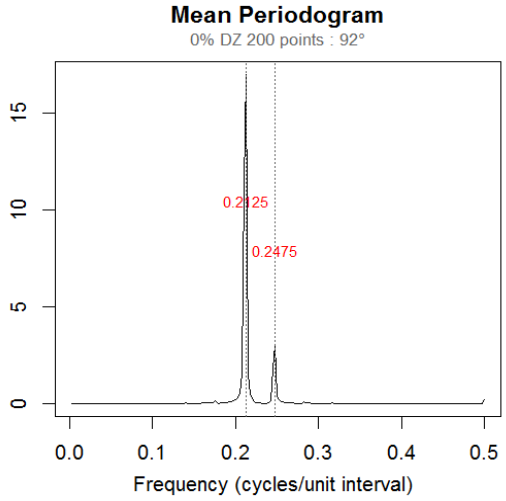

Fig. 8. Modulation effects of linear interpolation of waves sampled along θ = 92°. Signals: sin (2π 0.45 t) along 30°; noise: none.

Without related information of the spatial wave, the performance of interpolation algorithms is limited. However, if the background noises are high, the sampling errors are easier to smooth out as noises with linear interpolation method.

VI. Directional Sampling Errors in Reconstruction

Most sampling errors as defined by Eq. 1 can be easily filtered out in the process of reconstructing spatial waves with Fourier transform, especially with KZFT [1, 2, 7, 8]. This is because the Fourier transform and KZFT are highly selective: recovered movement energy decreases rapidly with bias from given frequencies. However, this method only works well for situations of low background noise. If noise level increases, the accuracy of reconstruction quickly decreases. One method to overcome this disadvantage is to average the reconstructed signal along the direction that perpendicular to its propagating direction. In this case, the spatial arrangement of the "phases" of directional sampling lines may cause a different type of sampling errors if the signal frequency isn't considered.

Fig. 9 is an illustration of the spatial phase patterns for a wave signal and its different reconstructions. The spatial interaction of signal and sampling errors generated patterns as if two waves moved in the field. Pattern 1 (bottom left) is for the sampling scheme using no frequency information, thus the sampling errors formed a "wave" propagating along y-axis, and this direction will not change with wave frequency.

The setting of directional sampling lines in Pattern 2 (bottom right) used wave frequency information, and its Moiré pattern direction will change with wave frequency. In Pattern 2, points in the connected regions with same color (white or red strips) are taken as if have the same wave phase, or are on the same sampling line along orthogonal direction and therefore could be averaged to filter out the noise.

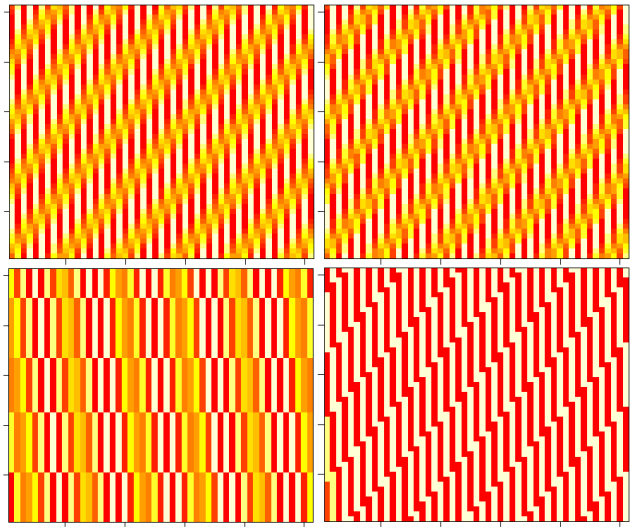

Fig. 9. Spatial patterns of a wave (upper left) and its reconstructions through averaging along orthognonal wave direction based on sampling of: (1) given direction (bottom left); (2) given direction and frequency (bottom right), (3) given direction, frequency, and fine averaging grain (upper right). The correlation coefficient with original signal (wave $sin(2\pi\cdot 0.45\cdot t)$ along 5°, no noise) is (1) 71.3%, (2) 72.5%, and (3) 99.6%, respectively.

Sampling scheme of Pattern 2 reflects the wave structure of signal; but since its averaging grain is too large, the accuracy of reconstruction is not high. Pattern 3 is improved by taking fine grain to average data. This improved sampling scheme can almost perfectly recover the signal even under strong noise.

Please notice that the best averaging grain is decided by noise level and the size of wave field. With higher noise levels we need more data points to average out the noise effects;

International Journal of Engineering Research & Technology (IJERT)
ISSN: 2278-0181
Vol. 5 Issue 12, December-2016

while with larger field size, there will be more points on the same sampling line and the rounding grain could be finer.

Also, the improved sampling scheme doesn't affect the sampling errors as defined by Eq. 1. In fact, Pattern 1, 2, and 3 have the same spectrum features for the sampling errors; and the sampling scheme of Pattern 1 is exact what we used for directional periodogram [6]. The relational of improved sampling scheme is to avoid introducing sampling errors caused by spatial phase shift.

VII. From Identification to Reconstruction

The reconstruction process used both wave direction and frequency information in the algorithm. The accuracy of the identified wave parameters directly affects the quality of reconstruction. Fortunately, as far as the identified parameters are not from a fake signal, optimization procedures can be used to improve their accuracy. During the optimization process, the highly selective feature decided by the frequency response characteristics of KZFT [2] helps to filter out unrelated moves and noise, and therefore we can accurately identify the real parameter based on given information of wave frequency and direction. For this reason, identification is the key step and important starting point for this process.

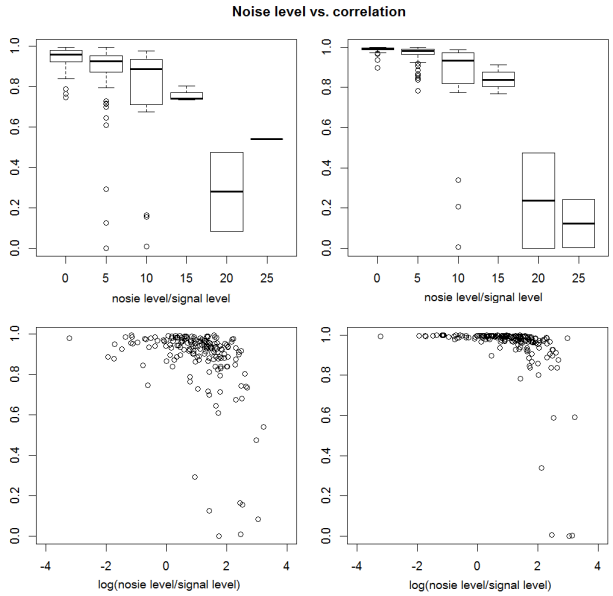

Fig. 10. Simulation results for correlation coefficients on different noise levels for 200 cases of 2D wave signals reconstructed based on identified wave parameters. (1) (upper left) Boxplot for reconstruction based on identified parameters; (2) (bottom left) Scatter plot for reconstruction based on identified parameters; (3) (upper right) Boxplot for reconstruction based on optimizated parameters; (4) (bottom right) Scatter plot for reconstruction based on optimizated parameters.

Our R package {kzfs} helps to realize the whole process from the step of identification to reconstruction. Function {kzpdr} is designed to collect directional periodogram data; estimation works will be done with function {kzpdr.eval} and {kzpdr.estimate}. {kzp2d} estimates wave parameters based on 2D periodogram. Function {OptDRP} and {Opt2DP} are given to optimize the identified parameters. For the reconstruction step, {kz.rc2} will recover wave movements in 2D field. Functions are also available for other auxiliary processes.

From the upper two Boxplots of Fig. 10, obviously, the correlation decreases when the noise levels increases, and the procedure usually fails to identify the wave parameters when the noise levels are more than 15 to 20 times of the signal levels. Comparing the two Scatter plots on the bottom, the quality of the reconstructions based on optimized parameters tends to be higher (about 5%) and is more robust when noise levels increases. The simulation was based on an automatic searching procedure utilizing KZ directional periodogram [6]. There are about 25 cases failed to be correctly identified because of extremely high noise ratio, very small field size, or being buried by other dominated signals.

The results illustrate that the whole procedure that from identification to reconstruction is feasible; and the optimization procedure is useful for improving the accuracy. Usually if the field size is large and the noise level is relatively low, the improvement of optimization is marginal. There are even few cases for which the reconstructions based on un-optimized parameters are slightly better than that of after optimization under extreme noisy conditions. But the effects of optimization are consistently positive for most cases under given setting.

VIII. Summary

The wave patterns formed by sampling errors are analogue to Moiré pattern formed by two sets of parallel lines, but has different underlying mechanism. In this paper, we discussed the sampling errors formed by the gridded wave field and its effects on the sampling lines along given direction. We have demonstrated that the sampling error is periodic signals with seesaw like wave; their fundamental frequency and dominated frequency are functions of the sampling direction. When the sampling errors act on the directional periodogram, the modulation effects can be predicted. We therefore are able to identify the source of these unusual periodogram spikes and do not take the incorrect spectral signals into the wave parameter identification analysis [6].

Generally speaking, the best way to avoid sampling error effects is to increase the sampling frequency so that the wave frequency will not be too close to 0.5. The second method is to smoothing the directional periodogram. This can be used to handle most of the cases in practice. When the wave frequency is high than 0.4, and the sampling errors cannot be smoothed out, we can predicate the modulated frequency spikes with Proposition 3. This method is useful for the identification of spatial wave parameters.

The formula to predict spectral behavior of sampling error effects have been used in our R package {kzfs} [7]. This package is designed for the separation and reconstruction of motion scales in 2D motion images on different directions based on KZ periodogram and KZFT. For the wave parameter identification, {kzfs} provides functions to check directional periodograms for spatial waves in the wave field. Results of this paper help to exclude the fraud spectral spikes caused by sampling errors of directional samples generated from the gridded data.

International Journal of Engineering Research & Technology (IJERT)
ISSN: 2278-0181
Vol. 5 Issue 12, December-2016

REFERENCES

[1] I. Zurbenko. The Spectral Analysis of Time Series. North-Holland Series in Statistics and Probability, 1986.
[2] W. Yang and I. Zurbenko. Kolmogorov–Zurbenko filters. WIREs Computional Statitics, 2:340–351, 2010.
[3] I. Zurbenko, M. Luo. Restoration of Time-Spatial Scales in Global Temperature Data. America Journal of Climate Change, 1(3): 154-163, 2012.
[4] I. G. Zurbenko, M. Luo. Surface Humidity Changes in Different Temporal Scales. America Journal of Climate Change, 4(3): 226-238, 2015.
[5] E. Weisstein. "Fourier Series--Triangle Wave." MathWorld. http://mathworld.wolfram.com/FourierSeriesTriangleWave.html
[6] M. Luo, I. Zurbenko, KZ Spatial Waves Separations, Journal of Research in Applied Mathematics, 3(4):1-7, 2017.
[7] M. Luo, I. Zurbenko. kzfs: Multi-Scale Motions Separation with Kolmogorov-Zurbenko Periodogram Signals. 2016.9.23. R package. https://CRAN.R-project.org/package=kzfs
[8] I. Zurbenko and A. Potrzeba-Macrina, Tides In The Atmosphere. Air Quality, Atmosphere and Health, 6(1):39–46, 2013.